

Semiempirical Characterization of Homonuclear Diatomic Ions: 5. The General Classification of Herschbach Ionic Morse Potential Energy Curves

Edward S. Chen* and Edward C. M. Chen

Center for High Performance Software, Rice University, 6100 S. Main, Houston, Texas 77005

Received: April 8, 2002; In Final Form: May 6, 2002

The Herschbach (*Adv. Chem. Phys.* **1966**, *10*, 310) classification of $XY(-)$ potential energy curves is updated. Using three independent binary metrics, there are eight (2^3) curves, expressed in a symmetrical notation as follows: $M(m)$ and $D(m)$, $m = 0$ to 3, where D and M signify **D**issociation and **M**olecular anion formation in a vertical electron impact, and m is the number of positive metrics. The metrics are the individual adiabatic and vertical electron affinities and the energy for dissociative electron attachment. Examples are the anions of: H_2 [$M(0)$, $D(0)$], O_2 [$M(2,1)$, $D(0)$], F_2 [$D(3,2)$], Na_2 [$M(2)$; $D(1)$], and I_2 [$M(3)$; $D(3,2)$]. Improved Morse curves for $H_2(-)$, $X_2(-)$, and $O_2(-)$ are calculated based on more accurate AE_a : F_2 , 3.02 ± 0.01 ; Cl_2 , 2.40 ± 0.01 ; Br_2 , 2.53 ± 0.01 ; I_2 , 2.52 ± 0.005 ; and O_2 , 1.07 ± 0.07 (all in eV). The AE_a for the main group homonuclear diatomic molecules are supported by periodic trends.

Introduction

The electron affinities, E_a , (positive for exothermic reactions) of many homonuclear diatomic molecules, E_2 have been measured but few Morse potential energy curves, MPEC are available. In the 1960s, Person and Herschbach estimated the Morse parameters for the halogen diatomic anions, $X_2(-)$.^{1,2} This paper is a part of a series in which curves for the $X_2(-)$, the rare gas positive ions, $Rg_2(+)$ and $O_2(-)$ were calculated from diverse data.^{3–7} This series was inspired by the classification of the Herschbach Ionic Morse Potential Energy Curves, HIMPEC. Nine types of $XY(-)$ potential energy curves, were identified based on **M**olecular anion formation or **D**issociation in a vertical transition, the sign of the $E_{\text{dea}} = E_a(X) - BDE_{XY}$ and vertical E_a , VE_a . The VE_a are the differences in the energy between the anions and the neutral in the neutral geometry. The E_a are the differences for the states in their most stable form. The largest E_a is the ground state or adiabatic E_a , AE_a . Due to ionic polarization forces, it is positive but E_a and VE_a can be either negative or positive.

The HIMPEC will be updated by adding the sign of the E_a as a classifier. This gives $2^3 = 8$ possible curve, described in a symmetrical notation: $M(m)$ and $D(m)$, $m = 0$ to 3, where m is the number of positive metrics. With the $r(e^-)$ - XY separation as a third dimension, eight subclasses $Mc(m)$ and $Dc(m)$ can be defined based on the **C**rossing of the polarization and covalent curves to give **M**olecular ions or **D**issociation. Improved Morse curves for multiple states of $H_2(-)$, $X_2(-)$, and $O_2(-)$ will be presented.

According to W. E. Deming “A systematic uncertainty or bias is never discovered, nor has any meaning, unless two or more distinct methods of observation are compared.”⁸ The AE_a for H_2 and N_2 are small but positive since the ground state is a polarization anion. The AE_a of many of the group IA, IB, III–VI, E_2 , have been measured by anion photoelectron spectroscopy, PES. However, only the following have been measured by a second technique: I_2 , 2.524, C_2 , 3.27 eV, Si_2 , 2.20 eV and S_2 , 1.67 eV.^{9,10} The AE_a (eV): F_2 , 3.02; Cl_2 , 2.40; Br_2 , 2.53 determined from the isoelectronic principle and O_2 , 1.07 determined from ion beam onsets have also been confirmed.¹⁰ The E_a for O_2 range from 0.15 to 1.07 eV.^{7,10–14} All data not

specifically cited come from ref 10. The random uncertainty is indicated by the subscripted integer. The systematic variation of the relative bond orders of $E_2(-)$ and E_2 will be examined to support the experimental AE_a .

Morse Potential Energy Curves

The Morse potentials for the neutral as referenced to zero energy at infinite separation and the HIMPEC are given by

$$U(X_2) = -2D_e(X_2) \exp(-\beta(r - r_e)) + 2D_e(X_2) \exp(-2\beta(r - r_e)) \quad (1)$$

$$U(X_2^-) = -2k_A D_e(X_2) \exp(-k_B \beta(r - r_e)) + k_R D_e(X_2) \exp(-2k_B \beta(r - r_e)) - E_a(X) + E(X^*) \quad (2)$$

where $D_e(X_2)$ is the spectroscopic dissociation energy, r is the internuclear separation, $r_e = r$ at the minimum of $U(X_2)$ and $E(X^*)$ is the excitation energy, $\beta = \nu_e(2\pi^2\mu/D_e[X_2])^{1/2}$, μ , is the reduced mass; k_A , k_B , and k_R is a dimensionless constant

$$D_e(X_2^-) = [k_A^2/k_R] D_e(X_2) \quad (3)$$

$$r_e(X_2^-) = [\ln(k_R/k_A)]/[k_B \beta(X_2)] + r_e(X_2) \quad (4)$$

$$\nu_e(X_2^-) = [k_A k_B/k_R^{1/2}] \nu_e(X_2) \quad (5)$$

$$-VE_a = D_e(X_2) (1 - 2k_A + k_R) - EA(X) + E(X^*) - 1/2 h\nu_e(X_2) \quad (6)$$

The Herschbach metrics E_{dea} , E_a and VE_a give k_A and k_R using eqs 3 and 6. A value of the frequency or r_e gives k_B from eqs 4 or 5 to define the HIMPEC. From eq 3 the relative bond order is $D_e(X_2^-)/D_e(X_2) = [k_A^2/k_R]$.

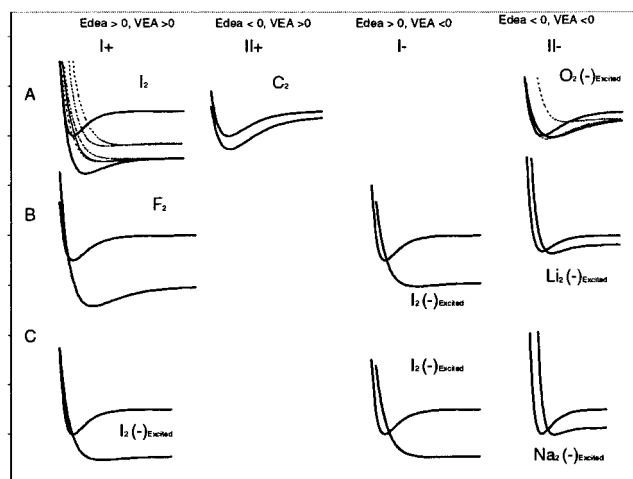


Figure 1. Reduced Morse potential energy curves illustrating original Herschbach classes.

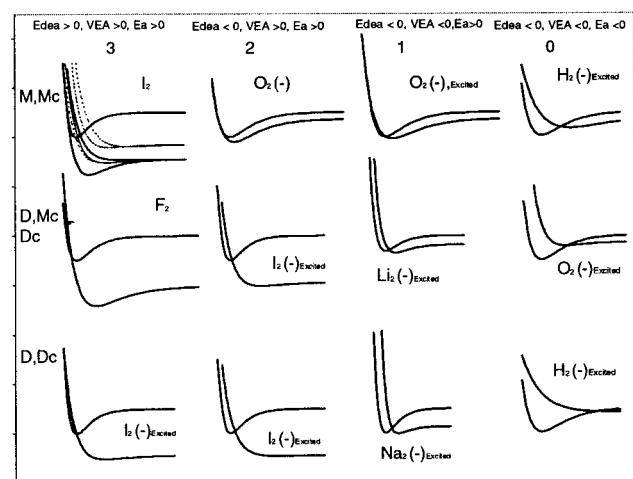


Figure 2. Reduced Morse potential energy curves illustrating modified Herschbach classes.

TABLE 1: Morse Parameters, Dimensionless Constants for Neutral Cation, and Anion Morse Potentials for E_2

| species | k_A | k_B | k_R | D_e (eV) | r_e (pm) | v (cm^{-1}) | E_a (eV) |
|-----------------------------|-------|-------|-------|------------|------------|--------------------------|------------|
| $\text{H}_2^+ 2\Sigma_u^+$ | 0.84 | 0.69 | 1.26 | 2.79 | 106 | 2250 | |
| $\text{He}_2^+ 2\Sigma_u^+$ | 1.11 | 0.62 | 2.40 | 2.58 | 108 | 1964 | |
| $2\Sigma_g^+$ | 0.16 | 0.49 | 1.38 | 0.08 | 190 | 300 | |
| H_2 neutral | 1.00 | 1.00 | 1.00 | 5.01 | 75.4 | 4395 | |
| H_2^- polarization | 1.00 | 1.00 | 1.00 | 5.1 | 75.4 | 4395 | |
| $2\Sigma_u^+$ | 1.07 | 0.53 | 2.14 | 2.58 | 145 | 1700 | |
| $2\Sigma_g^+$ | 0.12 | 0.56 | 0.99 | 0.05 | 280 | 285 | |
| $\text{O}_2 3\Sigma_g^-$ | 1.00 | 1.00 | 1.00 | 5.21 | 121 | 1580 | |
| $\text{O}_2^- 2\Pi_g$ | 1.09 | 0.85 | 1.30 | 4.78 | 129 | 1280 | 1.07 |
| $4\Sigma_u^-$ | 1.05 | 0.82 | 1.26 | 4.65 | 131 | 1210 | 0.95 |
| $2\Pi_u$ | 1.05 | 0.77 | 1.38 | 4.16 | 134 | 1089 | 0.45 |
| $2\Pi_u$ | 1.05 | 0.77 | 1.38 | 4.14 | 134 | 1089 | 0.43 |

Results and Discussion

Herschbach described the HIMPEC as follows: "A convenient qualitative classification of the types of $\text{XY}(-)$ potential energy curves which may occur are given in (Figure 1) The category I or II is determined from the sign of the E_{dea} . In both cases A and B, the free anion is bound, but for B as well as the unbound case C, the vertical transition leads to dissociation."² The "C" curves are slightly bound due to polarization forces. These are stronger than the attractions in He_2 but weaker than the interactions responsible for dipole bound anions of molecules such as cytosine, thymine, and uracil. Pseudo two-dimensional

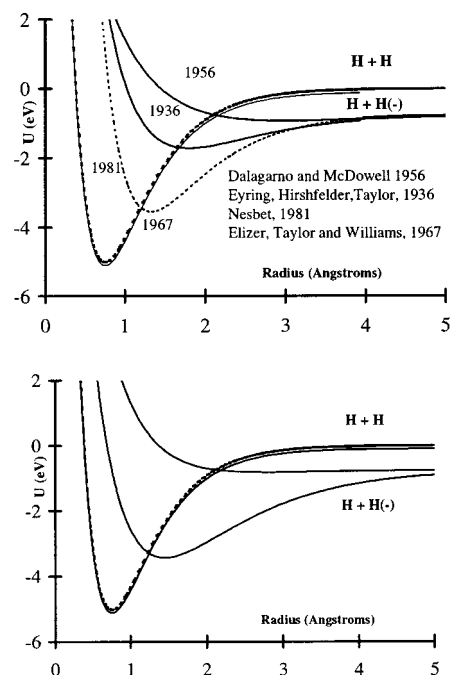


Figure 3. Morse potential energy curves for H_2 and its anions postulated theoretical and current "best" HIMPEC are shown for H_2 .

TABLE 2: Morse Parameters, Dimensionless Constants for Neutral and Anion Morse Potentials for X_2

| species | k_A | k_B | k_R | D_0 (eV) | r_e (pm) | v (cm^{-1}) | $-VE_a$ (eV) | $E(\text{abs})$ (eV) |
|-------------------------------|-------|-------|-------|------------|------------|--------------------------|--------------|----------------------|
| F_2 neutral | 1.00 | 1.00 | 1.00 | 1.60 | 141 | 917 | | |
| $\text{F}_2^- A 2\Sigma_u^+$ | 1.69 | 0.57 | 3.60 | 1.28 | 186. | 462 | -1.25 | |
| $B 2\Pi_{g3/2}$ | 0.56 | 0.66 | 2.76 | 0.18 | 259 | 140 | 1.10 | 1.63 |
| $B 2\Pi_{g1/2}$ | 0.45 | 0.56 | 2.58 | 0.12 | 267 | 119 | 1.16 | 1.71 |
| $C 2\Pi_{u3/2}$ | 0.40 | 0.66 | 3.57 | 0.07 | 340 | 72 | 2.84 | 2.67 |
| $C 2\Pi_{u1/2}$ | 0.46 | 0.60 | 3.89 | 0.09 | 322 | 85 | 3.18 | 2.62 |
| $D 2\Sigma_g^+$ | 0.51 | 0.45 | 5.64 | 0.07 | 355 | 74 | 5.92 | 3.67 |
| Cl_2 neutral | 1.00 | 1.00 | 1.00 | 2.52 | 199 | 565 | | |
| $\text{Cl}_2^- A 2\Sigma_u^+$ | 1.05 | 0.61 | 2.13 | 1.31 | 256 | 248 | -1.05 | |
| $B 2\Pi_{g3/2}$ | 0.42 | 0.63 | 2.29 | 0.19 | 334 | 99 | 2.58 | 1.63 |
| $B 2\Pi_{g1/2}$ | 0.26 | 0.76 | 2.00 | 0.08 | 331 | 79 | 2.66 | 1.64 |
| $C 2\Pi_{u3/2}$ | 0.32 | 0.64 | 3.22 | 0.08 | 376 | 65 | 5.47 | 2.40 |
| $C 2\Pi_{u1/2}$ | 0.44 | 0.60 | 3.59 | 0.14 | 371 | 79 | 5.97 | 2.65 |
| $D 2\Sigma_g^+$ | 0.39 | 0.65 | 4.88 | 0.08 | 391 | 65 | 9.51 | 3.32 |
| Br_2 neutral | 1.00 | 1.00 | 1.00 | 2.00 | 228 | 323 | | |
| $\text{Br}_2^- A 2\Sigma_u^+$ | 1.29 | 0.61 | 2.83 | 1.18 | 285 | 162 | -1.37 | |
| $B 2\Pi_{g3/2}$ | 0.43 | 0.60 | 1.90 | 0.20 | 354 | 61 | 0.73 | 1.19 |
| $B 2\Pi_{g1/2}$ | 0.29 | 0.55 | 2.06 | 0.08 | 412 | 36 | 1.63 | 1.62 |
| $C 2\Pi_{u3/2}$ | 0.35 | 0.64 | 3.32 | 0.07 | 410 | 39 | 3.95 | 1.87 |
| $C 2\Pi_{u1/2}$ | 0.58 | 0.61 | 4.41 | 0.15 | 398 | 55 | 5.66 | 2.41 |
| $D 2\Sigma_g^+$ | 0.51 | 0.60 | 5.77 | 0.09 | 436 | 41 | 8.67 | 3.18 |
| I_2 Neutral | 1.00 | 1.00 | 1.00 | 1.60 | 267 | 215 | | |
| $\text{I}_2^- A 1(1/2)$ | 1.18 | 0.65 | 2.23 | 1.01 | 321 | 110 | -1.70 | |
| $A 1(1/2)$ | 1.20 | 0.66 | 2.28 | 1.01 | 321 | 112 | -1.65 | |
| $B 1(3/2)$ | 0.46 | 0.66 | 1.51 | 0.23 | 365 | 53 | -0.52 | 0.84 |
| $B 1(3/2)$ | 0.58 | 0.68 | 2.40 | 0.23 | 380 | 55 | 0.53 | 0.95 |
| $B 1(1/2)$ | 0.22 | 0.56 | 2.02 | 0.04 | 480 | 19 | 1.07 | 1.52 |
| $B 1(1/2)$ | 0.25 | 0.57 | 2.32 | 0.04 | 480 | 20 | 1.47 | 1.59 |
| $C 1(3/2)$ | 0.38 | 0.66 | 2.88 | 0.08 | 434 | 32 | 1.95 | 1.64 |
| $C 1(3/2)$ | 0.40 | 0.68 | 3.18 | 0.08 | 434 | 33 | 2.37 | 1.71 |
| $C 2(1/2)$ | 0.62 | 0.60 | 3.13 | 0.19 | 413 | 45 | 2.55 | 2.22 |
| $C 2(1/2)$ | 0.66 | 0.63 | 3.59 | 0.19 | 413 | 48 | 3.14 | 2.50 |
| $D 2(1/2)$ | 0.49 | 0.45 | 3.62 | 0.11 | 508 | 25 | 3.73 | 3.07 |
| $D 2(1/2)$ | 0.53 | 0.47 | 4.15 | 0.11 | 504 | 26 | 4.48 | 3.22 |

HIMPEC for covalent and dipole bound states of cytosine and thymine have been calculated from experimental data.¹⁵

Reduced Morse Potential Energy curves r-HIMPEC illustrates the original classifications in Figure 1. The reduced curves are obtained by dividing the Morse potentials by the dissociation energy of the neutral and the radius by the internuclear distance of the neutral. Multiple curves are shown for $\text{I}_2(-)$ and $\text{O}_2(-)$ to illustrate the relationship between the various classes. The

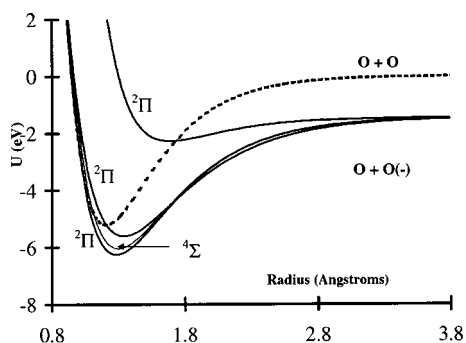


Figure 4. Morse Potential Energy Curves for O_2 and $O_2(-)$.

bold curves are the specific class. The ground state of $I_2(-)$ is $A[I+]$. The three $C_2(-)$ and ground-state $O_2(-)$ are $A[II+]$. The excited states of $O_2(-)$ are $A[II-]$ and $C[II-]$.

In Figure 2 the modified classifications are illustrated. All of the M curves are Mc curves but some of the D curves are Mc curves. The ground-state HIMPEC for Group IA are $M(2,3)$ and $Mc(2,3)$. The first excited states have been predicted and are $D(1)$. For $Li_2(-)$, the polarization curve crosses the first excited-state curve above the dissociation limit and is $Mc(1)$.

The $Na_2(-)$ crossing is below the dissociation limit making it $Dc(1)$.¹⁰ The Morse parameters and experimental data are in Tables 1 and 2.

Negative Ion States of H_2

The first step in assigning the experimental E_a to electronic states is the determination of the number of theoretical states. The H_2 anion has a polarization ground state and two covalent states. The ground state is a "neutral molecule plus free electron". Morse parameters (D , r , ν); 0.9 eV, 190 nm and 135 cm^{-1} and 0.16 eV, 300 nm, 600 cm^{-1} were calculated for the bonding and antibonding states in 1936 and 1956, respectively. The frequency in the 1956 curve is adjusted to give the experimental VE_a . In 1967 and 1981 improved bonding curves were calculated but the dissociation energy remained too small. The $H_2(-)$ like $He_2(+)$ and $H_2(+)$ has one bonding electron giving $D_e = 2.65$ eV. The curves shown in Figure 3, use the calculated frequency and internuclear distance with the predicted D_e for the bonding and polarization states.¹⁶⁻¹⁹

The ESR spectrum of the valence state anion has been recently observed in irradiated solid H_2 .²⁰ Two peaks are observed in the production of $H(-)$. The first has an abrupt

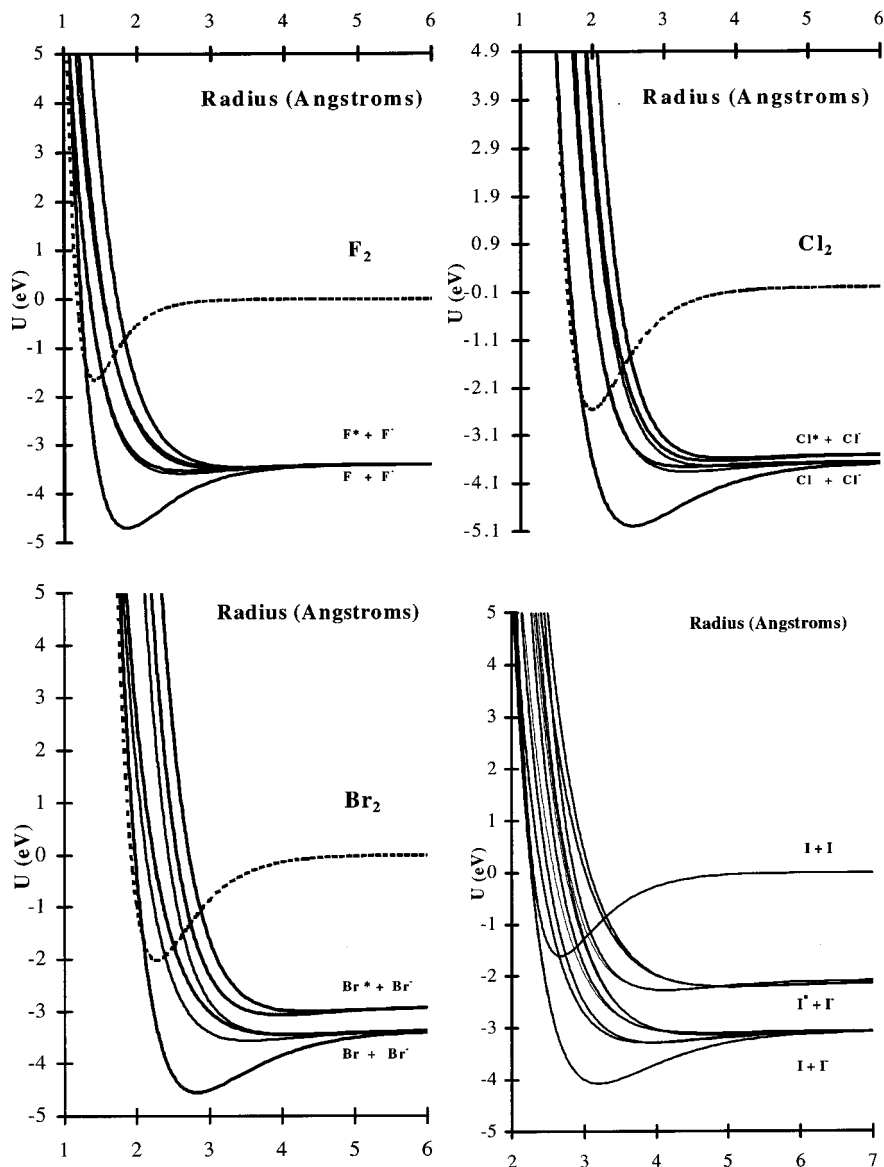


Figure 5. Morse Potential Energy Curves for $X_2(-)$ calculated from experimental data.

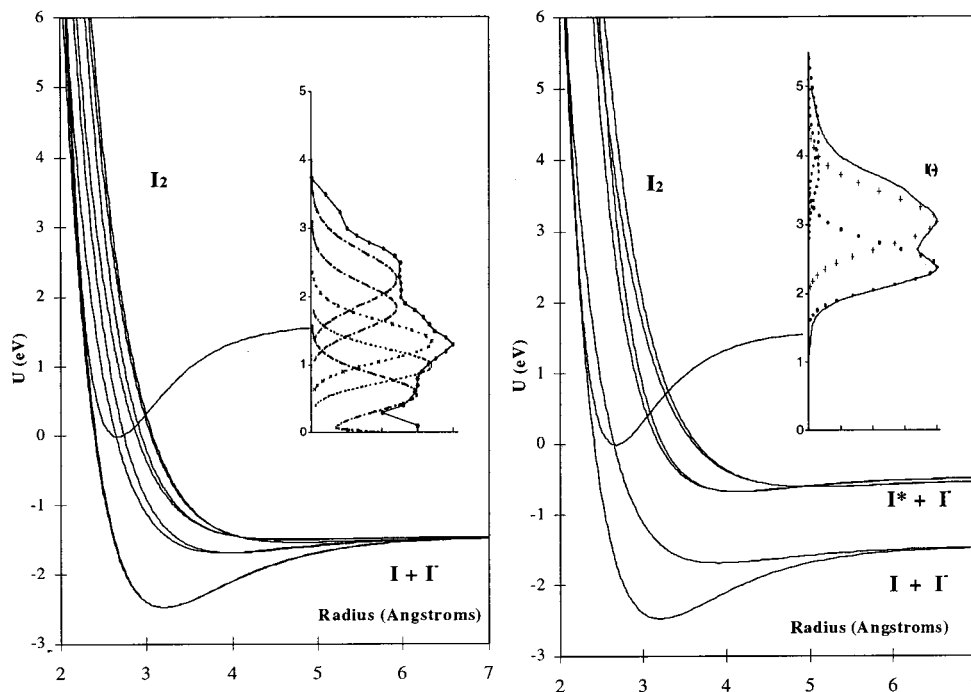


Figure 6. Morse potential energy curves for I_2 and $I_2(-)$ calculated from experimental data. $I(-)$ distributions calculated by the reflection method and experimental distributions from ref 26.

onset at the E_{dea} 3.75 eV, whereas the second an onset at 7 eV and a peak at 10 eV. Electron scattering data gives a VE_a of -2.8 eV for the lower state giving $r_e = 153$ pm and ν_e 1300 cm^{-1} .²¹ The size of the $H(-)$ is obtained from the $r_e - r(H) = 145 - 38 = 107$ pm. The $H(-)$ distribution and an assumed dissociation energy of 0.05 eV are used to calculate the excited valence state Morse potential. The bonding curve is an $M(0)$ curve, whereas the antibonding curve is a $D(0)$ curve. The similarity between the modified predicted and the “current best” curves shown in Figure 3 is striking.

The Negative Ion States of O_2

The superoxide anion was the first homonuclear diatomic anion to be observed. The experimental E_a are: [method, E_a (eV) and dates] photodetachment, 0.15, 1958; charge-transfer complexes, 0.75, 1961–71; electron swarm, 0.45, 1961; electron beam, 0.6, 1.1, 1961–71; alkali metal beam, 0.2, 0.3, 0.5, 0.8, 1.3, 1970–77; ion beam, 1.07, 70; PES, 0.43, 0.45, 1971–95 and ECD, 0.45, 0.5, 0.9, 1970–2002.^{10–14} In 1981, Michels calculated 11 E_a and predicted 24 states ($\Sigma [^2\Sigma_g^-(2), ^2\Sigma_u^-(2), ^4\Sigma_g^-(2), ^4\Sigma_u^-(2), ^2\Sigma_g^+, ^2\Sigma_u^+, ^4\Sigma_g^+, ^4\Sigma_u^+]$; $\Pi [^2\Pi_g(2), ^2\Pi_u(2), ^4\Pi_g(2), ^4\Pi_u(2)]$, and $\Delta [^2\Delta_g, ^2\Delta_u, ^4\Delta_g, ^4\Delta_u]$) leading to the lowest limit.²² The ground state $^2\Pi_g(3\sigma_g)^2, (1\pi_u)^4, (1\pi_g)^3, (3\sigma_u)^0$ or 2430 has an E_a , 1.07 eV which gives the dissociation energy. The frequency and radius were obtained from the electronic emission spectrum in solids.²³ The E_a , 0.95 eV is assigned to the $^4\Sigma$ state. The data give the Morse parameters 4.66 eV; 131 nm and 1230 cm^{-1} . The E_a , 0.43₀, 0.45₀ eV is assigned to the 2340 $^2\Pi$ state. The Morse parameters are well established. Morse parameters for the higher 1431 or 1341 $^2\Pi_g$ state have been reported. It has an E_a of -2.8 eV.²⁴

The ground and the first excited-state curves for $O_2(-)$ cross the neutral in the inverted Marcus region explaining the large activation energy. These are $M(2)$ because the E_a , and the VE_a are positive but the E_{dea} is negative and the molecular ion will be formed. The 2340 $^2\Pi$ curve and the ground-state neutral cross near the internuclear distance of the neutral. It is $M(2)$ or $M(1)$.

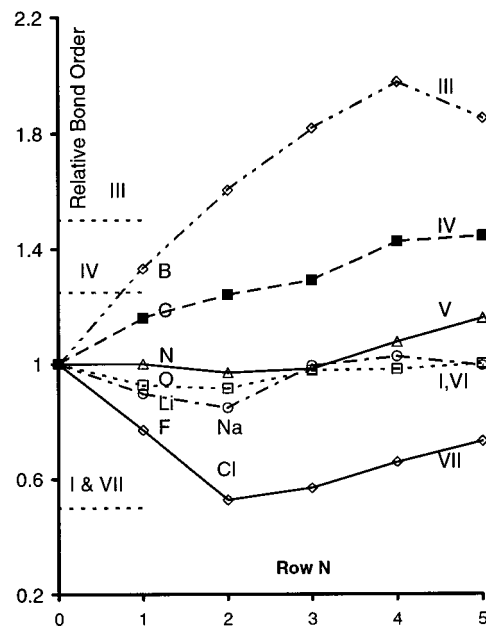


Figure 7. Relative bond order for homonuclear diatomic anions versus the row in the periodic table. The predicted bond orders are shown as horizontal lines for the Group I and VI, 0.5; Group IV, 1.25; and for the Group III, 1.5.

The higher $^2\Pi$ curve crosses the neutral curve at the internuclear distance of the anion. It is a $D(0)$ curve because all three metrics are negative and the vertical transition leads to dissociation. However, it is a $Mc(0)$ curve because the crossing with the polarization curve (not shown) leads to a molecular ion. Curves for the twenty four states of $O_2(-)$ will be calculated in a future part of this series.

Negative Ion States of X_2

Four primary negative ion states are predicted for $X_2(-)$. These are split into six states by spin–orbital coupling. The

six anion curves are split into twelve at the internuclear distance of the neutral.^{25,26} The procedure for obtaining the halogen curves has been described previously.^{3,4,6} The bond dissociation energies are obtained from the dissociation energies of the isoelectronic $Rg_2(+)$; the frequency has been measured and the internuclear distance can be calculated from the VE_a .

Twelve curves can be obtained for $I_2(-)$ because of the precise Morse parameters for the ground state, the large spin-orbital coupling and the resolved $I(-)$ distributions. The excited-state curves are determined from the experimental dissociation energies of the $Rg_2(+)$, the VE_a and the E_{abs} . In addition, the other Morse parameters for the $Rg_2(+)$ can be used as reference points. Figure 6 shows the agreement between the calculated and experimental distributions.²⁶ The ground-state curves for $Br_2(-)$ and $I_2(-)$ are M(3) and Mc(3), whereas those for $F_2(-)$ and $Cl_2(-)$ are D(3) and Mc(3). Except for the first excited states of $I_2(-)$ the excited-state curves are D(2) and Dc(2).

Systematic Variations in Morse Parameters

There are a number of consistencies in the dimensionless constants for the HIMPEC. In the ground-state curves, the k_A is greater than 1.0 indicating an increased attraction in the anion. However, the repulsive term, k_R is increased more than the attractive terms giving a smaller bond dissociation energy when the electron is added to an antibonding orbital. In the ground state of $C_2(-)$ where the electron goes into a bonding orbital, the values of k_A and k_R are comparable. The attractive terms for the excited states are less than 1.0. The frequency term, k_B is usually smaller than 1.0.

The AE_a of the main group homonuclear diatomic molecules are consistent with simple molecular orbital theory but the majority of relative bond orders are larger than predicted as shown in Figure 7. The relative bond order is approximately $D_e(X_2^-)/D_e(X_2) = [k_A^2/k_R]$. Because the ground states of $H_2(-)$ and $N_2(-)$ are polarization states the bond order is slightly greater than unity. The predicted value for Group I and VII is 0.5 but the values range from 0.55 to about 1.0. The AE_a of most of the Group I, V–VII homonuclear diatomic molecules are less than the AE_a of the atoms and the AE_a of the Group III and IV are greater than the AE_a of the atoms since their difference is equal to the difference in the dissociation energies. The largest increase in the dissociation energy is 2 eV for $C_2(-)$, whereas the largest decrease in the dissociation energy is 1.2 eV for $Cl_2(-)$. The average increase for the Group III and IV E_2 is 1 eV, whereas the average decrease for the $X_2(-)$ is 0.7 eV. The smooth changes across and down the periodic table support the experimental values of the AE_a of the main group elements and homonuclear diatomic molecules. The relative position of the group VI elements is especially significant since it supports the higher AE_a of 1.07 eV for O_2 .

Conclusions

The Herschbach classification of $XY(-)$ potential energy curves has been modified using the adiabatic and vertical electron affinities and the energy for dissociative electron

attachment as independent metrics. Eight (2^3) possible curves are expressed in a convenient symmetrical notation: M(m) and D(m), $m = 0$ to 3, where D and M signify immediate Dissociation and Molecular anion formation in a vertical transition, and m is the number of positive metrics. Eight subclasses can be defined as Mc(m) and Dc(m) by considering the crossing of the polarization curve with a covalent curve to lead to Molecular ions or to Dissociation. The following anions: $H_2[M(0),Mc(0);D(0),Dc(0)]$; $Li_2[M(2),Mc(2),D(1),Mc(1)]$; $O_2[M(2,1),Mc(2,1,0),D(0),Mc(0)]$; $F_2[D(3,2),Dc(3,2)]$; $Na_2[M(2),Mc(2);D(1),Dc(1)]$; and $I_2[M(3),Mc(3),D(3,2),Dc(3,2)]$ illustrate the classes. New ground and excited-state curves for $H_2(-)$ and $O_2(-)$ and the $X_2(-)$ are calculated based on improved data including the following AE_a : F_2 , 3.02 ± 0.01 ; Cl_2 , 2.40 ± 0.01 ; Br_2 , 2.53 ± 0.01 ; I_2 , 2.52_4 and O_2 , 1.07 ± 0.07 (eV). The AE_a for the Main Group homonuclear diatomic molecules are supported by periodic trends and simple molecular orbital concepts. However, the bond orders of many of the anions relative to that of the neutral are greater than predicted.

References and Notes

- (1) Person, W. B. *J. Chem. Phys.* **1963**, *38*, 109.
- (2) Herschbach, D. R. *Advances in Chemical Physics* **1966**, *10*, 250.
- (3) Chen, E. C.; Wentworth, W. E. *J. Phys. Chem.* **1985**, *89*, 4099.
- (4) Dojahn, J. G.; Chen, E. C.; Wentworth, W. E. *J. Phys. Chem. A* **1996**, *100*, 9649.
- (5) Chen, E. C.; Dojahn, J. G.; Wentworth, W. E. *J. Phys. Chem. A* **1997**, *101*, 3088.
- (6) Chen, E. S.; Chen, E. C. M. *Chem. Phys. Lett.* **1998**, *491*, 293.
- (7) Chen, E. S.; Wentworth, W. E.; Chen, E. C. M. *J. Mol. Struct.* **2002**, *606*, 1.
- (8) Deming, W. E. *The Statistical Adjustment of Experimental Data*; Dover: New York, New York, **1964**, p 11.
- (9) Zanni, M. T.; Taylor, T. R.; Greenblatt, B. J.; Soep, B.; Neumark, D. M. *J. Chem. Phys.* **1997**, *107*, 7613.
- (10) Christodoulides, A. A.; McCorkle, D. L.; Christophorou, L. G. *Electron Affinities of Atoms, Molecules and Radicals in Electron-Molecule Interactions and their Applications* Academic Press: New York, 1984; National Institute of Standards and Technology (NIST) Chemistry Web-Book, 2001. [http://webbook.nist.gov/].
- (11) Burch, D. S.; Smith, S. J.; Branscomb L. M. *Phys. Rev.* **1958**, *112*, 171.
- (12) Pack J. L.; Phelps, V. *Phys. Rev. Lett.* **1961**, *6*, 111.
- (13) Vogt, D.; Hauffe, B.; Neuert, H. Z. *Phys.* **1970**, *232*, 439.
- (14) Schiedt, J.; Weinkauff, R. Z. *Natforsch.* **1995**, *50a*, 1041.
- (15) Chen, E. S.; Chen, E. C. M. *J. Phys. Chem. B* **2000**, *104*, 7835.
- (16) Eyring, H.; Hirshfelder, J. O.; Taylor, H. S. *J. Chem. Phys.*, **1936**, *4*, 479.
- (17) Dalgarno, A.; McDowell, M. R. C. *Proc. Phys. Soc.* **1956**, *A69*, 617.
- (18) Elizer, I.; Taylor, H. S.; Williams, J. K. *J. Chem. Phys.* **1967**, *47*, 2165.
- (19) Nesbet, R. K. *Comments Atomic and Molecular Physics* **1981**, *11*, 25.
- (20) Ichikawa, T.; Tachikawa, H.; Kumada, T.; Kumagai, J.; Miyzaki, T. *Chem. Phys. Lett.* **1999**, *307*, 283.
- (21) Allan, M. *J. Phys. B* **1985**, *18*, L451.
- (22) Michels, H. H. *Adv. Chem. Phys.* **1981**, *65*, 227.
- (23) Rolfe J. *J. Chem. Phys.* **1964**, *40*, 1664.
- (24) Bailey, C. J.; Lavrich, D. J.; Serxner, D.; Johnson, M. A. *J. Chem. Phys.* **1996**, *105*, 1807.
- (25) Maslen, P. E.; Papanikolas, J. M.; Faeder, J.; Parson, R.; O'Neil, S. V.; *J. Chem. Phys.* **1994**, *101*, 5731.
- (26) Azria, R.; Abouaf, R.; Tellet-Billy, D. *J. Phys. B.* **1988**, *21*, L213.